Quantum 1/f Biochemical Detection Limits in THz Signatures Revealed by Scanning Tunneling Microscopy Currents

Amanda M. Truong, Peter H. Handel, *Senior Member, IEEE*, and Philip Fraundorf

***Abstract*—It may be possible to amplify the characteristic THz frequency oscillations of chemical and biological agents that contaminate surfaces or samples examined with the Scanning Tunneling Microscope (STM). This THz spectral signature of the biochemical molecules competes with the frequency fluctuations introduced as phase noise close to the examined THz frequency by the 1/f fluctuations of the tunneling resistance, of the resistance of the STM tip, and of the spreading resistance in the sample. Indeed, as we show below, the achievable spectral sensing resolution is $\Delta\omega/\omega = [2\ \mathrm{C}\ \ln 2]^{1/2} = [2\ \ln 2(S_R/R^2)/4Q_l^4]^{1/2} = [1.66\cdot 10^{-12}]^{1/2} = 1.3\cdot 10^{-6}$.**

Therefore, we have calculated the quantum $1/f$ noise of STMs for the first time, also determining the STM image resolution limits, including both the conventional and coherent quantum 1/f (Q1/f) effects. The main contributions are found to be quantum 1/f tunneling current noise, and quantum 1/f effect in the piezoelectric transducers in the feedback loop that controls the position of the needle above the sample. The results are compared with experimental data on STM resolution.

***Index Terms*—Phase noise, quantum 1/f noise (Q1/f), spectral sensing of biochemical agents, scanning tunneling microscope (STM) quantum limitations, STM resolution limits, 1/f noise.**

I. Introduction

THE quantum 1/f (Q1/f) resolution limits imposed by Q1/f noise [1]–[11] on Scanning Tunneling Microscopes (STMs) are determined here for the first time, including both the conventional and coherent Q1/f effects. Several noise contributions are considered. When the tip or needle is stationary, the main contribution is found to be Q1/f tunneling noise. This tunneling current noise contains contributions from the tunneling process through the vacuum, from the needle itself, and from the spreading resistance in the sample. The conventional and coherent Q1/f effects and their connection are briefly described and calculated. The resulting Q1/f formulas are used to derive the 1/f noise in each component, which is then compared with experimental data [12]. Finally, the Q1/f noise is shown to mimic fluctuations in the tip-sample separation distance, which ultimately limits the resolution of the STM. The fluctuations introduced by the piezoelectric feedback loop when the needle is scanning the sample are considered in the Appendix of a companion paper [13].

Manuscript received August 6, 2007; revised February 19, 2008; accepted February 26, 2008. The work was supported in part by the Army Research Office and Army Research Laboratory. The associate editor coordinating the review of this paper and approving it for publication was Dr. Dwight Woolard.

The authors are with the Department of Physics and Astronomy and the Center for Nanoscience, University of Missouri–St. Louis, St. Louis, MO 63121 USA (e-mail: am.troung@hotmail.com; handel@umsl.edu).

Digital Object Identifier 10.1109/JSEN.2008.923214

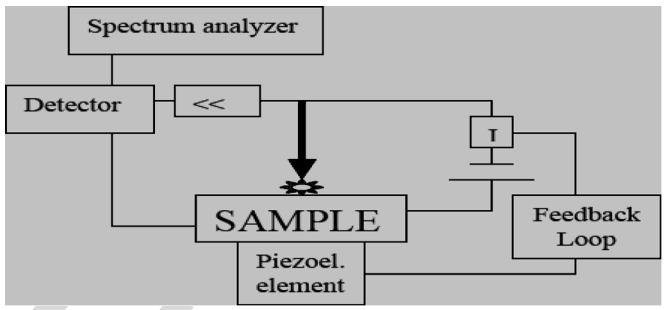

Fig. 1. Biochemical THz signatures revealed by scanning tunneling microscopy currents.

To find the quantum limits to the amplification of the characteristic THz frequency oscillations of chemical and biological agents that contaminate surfaces or samples examined with the STM, we propose to proceed as follows.

In the tungsten tip T (Fig. 1), a preliminary calculation of the coherence parameter s indicated that both coherent and conventional Q1/f effects affect the resistance, with weights determined by the coherence parameter $s = 5.6\cdot 10^{-13}\ \mathrm{cm}\cdot N'$; Here, N' is the number of electrons per cm in the direction of the current. A detailed calculation of the 1/f noise contributions in the tip yields analytical expressions for the spectral density of fractional resistance fluctuations $\delta R_t/R_t$. For a tungsten tip cone angle of 7.5°, minimal radius of 100 Å, total length of 15 μ, one obtains $S_{dRt/Rt} \cong 10^{-10}/f$.

In the vacuum through which the electrons tunnel, $s \ll 1$ and only conventional Q1/f effect is present. We obtain in this case, with a potential barrier of $U = 0.1$ eV, tunneling current of 20 pA, and a tunneling gap of $3\cdot 10^{-10}$ m modulated by the agent's molecules

$$S_{\delta R_v/R_v}(f) = \frac{4\alpha}{3\pi f N}\frac{(\Delta v)^2}{c^2} = \frac{4.8\times 10^{-8}}{f}. \quad (1)$$

In the sample, the Q1/f effect in the spreading resistance is mainly coherent, with small conventional contributions. The sample in [12] is a silver film, thickness 50 nm, evaporated on a silicon wafer

$$S_{\delta R_s}(f) = \frac{1}{1+s}S^{\mathrm{conv}}_{\frac{\delta R_s}{R_s}}(f)\cdot R_s^2 + \frac{s}{1+s}S^{\mathrm{coh}}_{\frac{\delta R_s}{R_s}}(f)\cdot R_s^2 = \frac{5.6\cdot 10^{-5}\Omega^2}{f}. \quad (2)$$

Within the silver sample (see Fig. 1), we have $dN = n_{\rm Ag}{\rm dV} = n_{\rm Ag}2\pi r^2 dr$, and the coherence parameter is $s = N' r_o = 4\pi r_o n_{\rm Ag} r^2$; here, $r_o = e^2/{\rm mc}^2 = 2.8\ 10^{-13}$ cm = classical radius of the electron, N' is the number of electrons per cm.

The total resulting resistance R (and current at constant applied V) fluctuations are thus given by

$$\begin{aligned} S_{\frac{\delta R}{R}}(f) &= S_{\frac{\delta I}{I}}(f) \\ &= \left(\frac{R_t}{R}\right)^2 S_{\frac{\delta R_t}{R_t}}(f) + \left(\frac{R_v}{R_{\rm total}}\right)^2 S_{\frac{\delta R_v}{R_v}}(f) \\ &\quad + \left(\frac{R_s}{R_{\rm total}}\right)^2 S_{\frac{\delta R_s}{R_s}}(f) \\ &= \frac{4.8\times 10^{-8}}{f}. \end{aligned} \tag{3}$$

With tunneling exponent per unit length $\kappa = [(2\ {\rm mU})^{1/2}]/\hbar$, and quality factor of the THz oscillation loop $Q_l = 10$, this yields an error ds_o in the determination of the height of the sample, and a frequency noise $S_{\delta\omega/\omega}$

$$\delta s_0 = \frac{\delta I}{I}\frac{1}{2\kappa} = \frac{5.5\times 10^{-15}\ {\rm m}}{\sqrt{\rm Hz}} \tag{4}$$

$$\begin{aligned} {\rm S}_{\delta\omega/\omega} &= ({\rm S}_{\mathbf{R}}/{\rm R}^{\mathbf{2}})/4{\rm Q}_{\mathbf{l}}^{\mathbf{4}}{\rm f} = 4.8\cdot 10^{\mathbf{-8}}/4\cdot 10^{\mathbf{4}}{\rm f} \\ &= 1.2\cdot 10^{\mathbf{-12}}/{\rm f} = {\rm C/f} \end{aligned}$$

or phase noise

$$\begin{aligned} \mathbf{L(f)} &= \mathbf{10}\log\left[(\mathbf{1/2})(\boldsymbol{\omega}/\mathbf{2\pi f})^{\mathbf{2}}\mathbf{S}_{\boldsymbol{\delta\omega\omega}}\mathbf{(f)}\right] \\ &= \mathbf{27\ dBc} \quad @{\rm f} = 1\ {\rm kHz} \end{aligned}$$

for $\omega/2\pi = 1$ THz.

The achievable THz spectral resolution is therefore, as shown in detail below

$$\begin{aligned} \Delta\omega/\omega &= [2{\rm C}\ln 2]^{1/2} = \left[2\ln 2({\rm S}_{\mathbf{R}}/{\rm R}^{\mathbf{2}})/4{\rm Q}_{\mathbf{l}}^{\mathbf{4}}\right]^{1/2} \\ &= [1.66\cdot 10^{\mathbf{-12}}]^{1/2}. \\ \mathbf{L(f)} &= \mathbf{10}\log\left[(\mathbf{1/2})(\boldsymbol{\omega}/\mathbf{2\pi f})^{\mathbf{2}}\mathbf{S}_{\boldsymbol{\delta\omega\omega}}\mathbf{(f)}\right] \\ &= 27\ \mathbf{dBc} \quad @{\rm f} = 1\ {\rm kHz}. \end{aligned}$$

II. Theory

The STM operates using the principles of quantum tunneling; in effect it measures the topography and electron distribution on the sample surface. When a voltage is applied, the electrons tunnel across the gap from the negatively charged tip to the positively charged sample. These electrons create a tunneling current which completes a feedback loop in the circuit. The feedback loop maintains a constant current throughout the circuit in the scanning mode, while the tunneling resistance varies. A computer then relates the resulting voltage on the piezoelectric to the tip height above the sample, which is controlled by a piezoelectric crystal, and produces a representative image of the surface. Images can be obtained using one of two methods: maintaining constant height above the sample and producing an image as a function of the varying tunneling current, or by maintaining a constant tunneling current and producing an image as a function of varying tip height. The fluctuations in the tunneling current or voltage fluctuations in the piezoelectric crystal result in deviations in tip-sample separation distance.

Here, we consider only a basic STM circuit with the needle kept stationary, disconnected from the feedback loop in order to find the ultimate limitations achievable with an STM with manual control or with an ideal feedback loop. The important effect of the noise in the piezoelectric feedback loop is considered elsewhere. The circuit consists of three components. The first region of interest, i.e., generating 1/f noise, is the tip, which in this case is tungsten. The second region is the space between the tip and sample, which we refer to as the vacuum, where the tunneling occurs. Finally, the sample, which consists, e.g., of a silver film deposited onto silicon. Note that the current fluctuations calculated for this stationary case yield equivalent height fluctuations when the current is held constant by an ideal, noiseless feedback loop that raises and lowers the stationary needle automatically. The case of the scanning needle is treated separately in a companion paper on piezoelectric positioning fluctuations limiting the resolution of the STM in the scanning mode.

In each region, the resistance fluctuations, or equivalently, the resulting current or voltage fluctuations, can be described by either the conventional or coherent Q1/f formulas, in general, by the universal Q1/f formula, containing the s parameter [1]–[5]. The expression for the power spectral density of fractional fluctuations given by the coherent Q1/f effect is

$$S_{\frac{\delta R}{R}}^{\rm coh}(f) = \frac{2\alpha}{\pi f N} \tag{5}$$

and the spectral density caused by the fundamental cross section and rate fluctuations described by the conventional 1/f effect is

$$S_{\frac{\delta R}{R}}^{\rm conv}(f) = \frac{4\alpha}{3\pi f N}\left(\frac{\Delta v}{c}\right)^2 \tag{6}$$

where $\alpha = {\rm e}^2/\eta{\rm c} = 1/137$ is the fine structure constant, N is the number of carriers, $\Delta\mathbf{v}$ is the velocity change of the carriers in the process considered, and c is the speed of light. Both aspects are combined in the general Q1/f formula

$$S_{\frac{\delta R}{R}} = \frac{1}{1+s}S_{\frac{\delta R}{R}}^{\rm conv}(f) + \frac{s}{1+s}S_{\frac{\delta R}{R}}^{\rm coh}(f) \tag{7}$$

where the coherence parameter

$$s = 2N' r_0 \tag{8}$$

indicates to what extent the energy of the drift motion of the electrons adds up coherently or conventionally over the cross section of the current, in the Hamiltonian [5]. We denoted with N' the number of carriers per unit length in the direction of the current flow, and with

$$r_0 = \frac{e^2}{4\pi\varepsilon_0 mc^2} = 2.82\times 10^{-15}\ {\rm m} \tag{9}$$

the classical radius of the electron, where $\varepsilon_{\rm o}$ is the vacuum permittivity. Often, the dominant form of 1/f noise occurring in each region can be determined, based on the number of current carriers in the region allowing for cancellation of one of the terms in the general formula. The coherent form of 1/f noise dominates regions with an abundance of current carriers. After the fractional fluctuations have been calculated, the spectral

TABLE I
PARAMETERS FOR THE TUNGSTEN TIP

Parameter	Value used	Unit
Tip cone angle (γ)	7.5	Degrees
Minimal tip radius (a)	$1x10^{-8}$	Meters
Distance from cone vertex (r_{min})	$7.6x10^{-8}$	Meters
Total length (r_{max})	$1.5x10^{-5}$	Meters
Tungsten density (ρ)	19.25	g/cm^3
Concentration (n_w)	$6.3x10^{28}$	$Molec/m^3$
Number of carriers (N)	$3.8x10^{12}$	Molec
Current (I)	$2x10^{-11}$	Amps
Resistivity (ρ_w)	$5.6x10^{-8}$	Ωm

density in each region can be obtained using the following relation:

$$S_{\delta R} = R^2 \cdot S_{\frac{\delta R}{R}}(f). \tag{10}$$

The resistance fluctuations from each region are uncorrelated, contributing independently to the total spectral density of resistance fluctuations of the whole circuit. Ultimately, these resistance fluctuations can give insight into height variations between tip and sample, interpreted as noise in STM images.

III. TUNGSTEN TIP NOISE CONTRIBUTION CALCULATION

The STM tip is perhaps the most important component; the sharper and more durable the tip, the more accurately it can interpret the sample surface. STM tips have been made from a wide variety of materials, from platinum-iridium to carbon nanotubes. The size of the tip also varies greatly, depending on its composition, and can be as narrow as a few hundred angstroms. Narrower tips are advantageous because they can detect more subtle surface features. For this calculation, we consider a tungsten tip with typical narrow cone geometry. The vector $\mathbf{r}$, which runs along the cone axis, is used to define the solid angle and has its origin at the hypothetical tip of the cone. The tip is represented here with cone angle γ defining the angle between the center axis of the tip and the sidewall. Of course, the tip cannot have an infinitely sharp point; an actual STM tip is blunted at the end. Taking this into consideration, we assume the blunted tip end has a finite radius $a = 100$ angstroms. Also, because the end is blunted, the beginning of the tungsten tip is not at the vertex of the cone, it actually begins some finite distance up from the vertex. Using simple geometry, if the cone angle is 7.5° and the small end of the tungsten tip has a radius of 100 angstroms, then the tip itself will begin 760 angstroms from the vertex of the cone. For all further calculations, this distance of 760 angstroms will be called $r_{\min}$ and the total length of the tip will called $r_{\max}$.

For convenience, the parameters for the tungsten tip [12] that are used in the following calculations have been tabulated in Table I.

First, the concentration of current carriers within the tip is calculated to reveal the dominant form of 1/f noise in the region. The number of carriers N in the tungsten tip is equal to the concentration times the total volume, and can be written in integral form as

$$N = \int n_w \cdot dV. \tag{11}$$

The concentration n_w for the tungsten tip is the product of the density, the inverse atomic mass number and the Avogadro number, which gives the concentration in atoms, or electrons, per cubic meter. The concentration for tungsten is $n_w = 6.3 \times 1028$ molecules per cubic meter. Next, we formulate the differential volume element in the tip region $dV = Adr$. For the tip with cone geometry, we assume the cone angle γ to be small and the end of the tip having a finite small radius a. The area element is obtained by calculating the solid angle

$$\Omega^t = \iint \frac{\hat{n} \cdot da}{r^2} = \iint \sin\theta d\theta d\varphi = 2\pi(1 - \cos\gamma) \tag{12}$$

where the limits of integration for φ are from 0 to 2π, and for θ are 0 to $\alpha/2$. Now, the volume element becomes

$$dV^t = Adr = (\Omega r^2)dr = 2\pi(1 - \cos\gamma)r^2 dr. \tag{13}$$

The average number of carriers in the tip is found by integrating over the volume in (11), letting the length range from $r_{\min}$ to $r_{\max}$

$$\langle N \rangle^t = 2\pi(1 - \cos\gamma) \cdot n_w \frac{1}{3}\left[r_{\max}^3 - r_{\min}^3\right]. \tag{14}$$

Now, using the concentration and radial length values found in the above table, we have

$$\langle N \rangle^t = 3.8 \times 10^{12} \text{ atoms}. \tag{15}$$

This number represents the total number of atoms in the entire tip. The average number of carriers per unit length is then

$$N' = \langle N \rangle^t / r_{\max} = 2.5 \times 10^{17} \frac{\text{molec}}{m} \tag{16}$$

which gives a coherence parameter of

$$s = 2r_0 N' = 1410. \tag{17}$$

With this fairly large number of carriers, the coherent form of Q1/f noise is dominant in the tungsten tip. It is important to note that because of its unique geometry, the tip exhibits both coherent and conventional Q1/f fluctuations. In the small region at the narrow end of the tip, there are fewer carriers present and therefore, this region could perhaps exhibit conventional 1/f fluctuations. In fact, the number of carriers per unit length multiplied with the classical radius r_0 always yields a parameter s larger than unity. Moving towards the base, the tip becomes broader, more carriers are available, so these thicker regions towards the base are dominated by coherent 1/f fluctuations. In such regions, the concentration of carriers is uncertain, therefore, spectral density is formulated using both coherent and conventional terms, and also involving the coherence parameter s.

TABLE II
PARAMETERS FOR THE VACUUM

Parameter	Value used	Unit
Tunneling distance (s_0)	$2\text{x}10^{-10}$	M
Carrier energy (W_e)	1	EV
Carrier mass (m)	$9.1\text{x}10^{-31}$	Kg
Carrier velocity (v)	$5.9\text{x}10^{5}$	m/s
Number of carriers (N)	1	
Current (I_t)	$2\text{x}10^{-11}$	A

The resistance of the tungsten tip, the so-called "spreading resistance," is now calculated. Knowing the resistivity ρ_w, we integrate over consecutive "shells" of increasing radial distance from the cone vertex, eventually covering the entire length of the tip

$$R_t = \int \frac{\rho_w dr}{A} = \int_{r_{\min}}^{r_{\max}} \frac{\rho_w dr}{2\pi(1-\cos\gamma)r^2} = 14.2\,\Omega. \quad (18)$$

Finally, the spectral density of resistance fluctuations in the tungsten tip is calculated using the generalized Q1/f formula and the coherence parameter s

$$S_{\delta R_t}(f) = \frac{1}{1+s} S^{\text{conv}}_{\frac{\delta R_t}{R_t}}(f) \cdot R_t^2 + \frac{s}{1+s} S^{\text{coh}}_{\frac{\delta R_t}{R_t}}(f) \cdot R_t^2. \quad (19)$$

Within the tungsten tip, we have

$$dN = dV \cdot n_w = 2\pi(1-\cos\gamma)r^2 dr \cdot n_w \quad (20)$$

and the coherence parameter is

$$s = 2r_0 \frac{n_w dV}{dr} = 4\pi r_0 n_w (1-\cos\gamma) r^2. \quad (21)$$

Now, our expression for the spectral density becomes

$$S_{\delta R_t}(f) = \frac{\rho_w^2 \alpha \left(\frac{\Delta v}{c}\right)^2}{f 6\pi^4 (1-\cos\gamma)^3 n_w} \int_{r_{\min}}^{r_{\max}} \frac{dr}{[1+Hr^2]r^6} + \frac{\rho_w^2 \alpha r_0}{f\pi^3(1-\cos\gamma)^2} \int_{r_{\min}}^{r_{\max}} \frac{dr}{[1+Hr^2]r^4}. \quad (22)$$

where we have used $\text{H} = 4\pi \text{r}_0 n_w (1-\cos\gamma)$ to simplify the integral.

At this point, the spectral density can be simplified by considering two cases; when r is very small, near the point of the tip, and when r is large, towards the base of the tip. In the first case, when r is small, the denominator of the first integral is dominated by the r^6 factor. When r is very large, the denominator of the second integral is dominated by the r^4 factor. Therefore, the above equation is simplified by dropping the $[1 + \text{H r}^2]$ factor in the denominators completely, leaving

$$S_{\delta R_t}(f) = \frac{\rho_w^2 \alpha \left(\frac{\Delta v}{c}\right)^2}{f 6\pi^4 (1-\cos\gamma)^3 n_w} \int_{r_{\min}}^{r_{\max}} \frac{dr}{r^6} + \frac{\rho_w^2 \alpha r_0}{f\pi^3(1-\cos\gamma)^2} \int_{r_{\min}}^{r_{\max}} \frac{dr}{r^4}. \quad (23)$$

In the tungsten tip, assuming random collisions of the carriers with the lattice, we have

$$\left(\frac{\Delta v}{c}\right)^2 = \frac{6k_B T}{m^* c^2} = 2.9 \times 10^{-6} \quad (24)$$

where m^* is the effective mass of the charge carrier in the tungsten tip. For simplicity, we have set $m^* = 0.1\, m_e$, which is an average value for the effective mass of the electron in most semiconductor materials. With all of the parameters defined, we evaluate the expression of the spectral density

$$S_{\delta R_t}(f) = \frac{2.24 \times 10^{-13}\,\Omega^2}{f} + \frac{2.2 \times 10^{-8}\,\Omega^2}{f}. \quad (25)$$

Clearly, the second term, the coherent contribution dominates in the tungsten tip region. The fractional fluctuations in resistance are obtained by dividing the spectral density by the squared tip resistance

$$S_{\frac{\delta R_t}{R_t}}(f) = S_{\delta R_t} \cdot R_t^{-2} = \frac{1.1 \times 10^{-10}}{f}. \quad (26)$$

IV. VACUUM SPACE NOISE CONTRIBUTION CALCULATION

The space between the tip and the sample, referred to as the vacuum, is the region where the tunneling occurs. By applying a voltage between the tip and the surface, the electrons in the conducting tip are attracted to the positive ions in the sample. If the tip is brought within a relatively close proximity to the surface, the electrons will tunnel from the tip to the surface. The current of electrons tunneling from tip to sample depends strongly on this separation distance, and for separation distances greater than 1 nm, no tunneling occurs.

The parameters [12] used in the following calculations for the vacuum space are tabulated in Table II

Now, the number of carriers N in the tunneling current must be calculated. In general, an electric current can be expressed in terms of the concentration of carriers, the drift velocity and the cross sectional area of the current: $I = nqv_dA$. Rewritten in terms of s_0, the distance between the tip and the sample, and with $N = N'\ s_0 = nA\ s_0$, the current that passes through the vacuum space is

$$I_t = eN(v_d/s_0). \quad (27)$$

Solving this expression for N, the number of carriers, gives

$$N = \frac{I_t s_0}{e v_d} \quad \text{or} \quad N' = \frac{I_t}{e v_d}. \quad (28)$$

Now, we can substitute values for the tunneling current I_t, and tunneling distance s_0, given by Koslowski [12] as 20 pico-amps and two angstroms, respectively. The energy of carriers is only on the order of a couple electron volts, because the carriers come from the Fermi sphere of the tungsten tip. From classical mechanics, the energy is proportional to the velocity squared. If

we set the energy of the carriers, W_e, to 4 eV, which is an average value for the Fermi energy in most metals, the velocity can be solved for

$$v_d = \sqrt{\frac{2(W_e)}{m_e}} = 1.2 \times 10^6 \text{ m/s} \tag{29}$$

where m_e is the mass of the carrier, the electron. Converting electron volts to joules, we obtain a velocity for the electrons as they move through the vacuum space between the tip and sample. Now, the number of carriers N in the vacuum is obtained

$$\langle N \rangle^v = \frac{I_t s_0}{e v_d} = 2.1 \times 10^{-8} \text{ molecules.} \tag{30}$$

Per unit length we get $N' \approx 100/\text{m}$ and, therefore, obtain $s = 2r_0 N' \approx 10^{-12} \ll 1$. So, when calculating the resistance fluctuations of the tunneling current, the number of carriers N will be set to one. The conventional form of Q1/f noise, therefore, dominates the tunneling current, because of the limited number of carriers.

Next, we calculate the tunneling resistance, which is more complex in this region, and must be obtained through an expression for the tunneling current used in combination with Ohm's law. This time the expression for the current should include a decaying exponential term to describe the tunneling process more accurately. The tunneling current can be written

$$I_v(t) = I_0 e^{-2\kappa s_0} \tag{31}$$

where I_0 is the tunneling current, s_0 is the distance between the tip and the sample, and κ is given by

$$\kappa = \frac{\sqrt{2mU}}{\hbar}. \tag{32}$$

The exponential term in the expression is called the transmission coefficient, the probability that the electron will tunnel through the vacuum space.

Before calculating the tunneling resistance in the vacuum, we first write the variance in the vacuum current by differentiating both sides, and then dividing by the vacuum current

$$\frac{\delta I}{I} = -2(\delta\kappa)s_0. \tag{33}$$

The variance in kappa $\delta\kappa$ is found in a similar fashion

$$\delta\kappa = \frac{1}{2}\frac{(2mU)^{-\frac{1}{2}}}{\hbar} \cdot 2m\delta U \tag{34}$$

which gives

$$\frac{\delta\kappa}{\kappa} = \frac{1}{2}\frac{\delta U}{U}. \tag{35}$$

Now, our expression for the vacuum current variance becomes

$$\frac{\delta I}{I} = -s_0\kappa\frac{\delta U}{U}. \tag{36}$$

TABLE III
PARAMETERS FOR THE SILVER SAMPLE

Parameter	Value used	Unit
Silver density (ρ)	10.49	g/cm^3
Concentration (n_{Ag})	5.86x10^{28}	Molec/m^3
Number of carriers (N)	1.5x10^7	Molec
Current (I)	2x10^{-11}	Amps
Resistivity (ρ_{Ag})	1.59x10^{-8}	Ωm
Initial tunneling distance (r_i)	1x10^{-10}	Meters
Silver film thickness (r_f)	5x10^{-8}	Meters

We let U represent the potential barrier $U = V + C$, where C is some constant. At this point, we can utilize Ohm's Law to write an expression for the differential resistance in the vacuum space

$$R_v = \frac{\delta V}{\delta I} = \frac{U}{I s_0 \kappa}. \tag{37}$$

For most applications, kappa has a value of 20–25 nm^{-1}, here we use the lower limit of 20 nm^{-1}. The other values are obtained from the experimental data: the potential barrier U of 0.1 V, tunneling current of 20 pA, and tunneling distance of 200 pm. Applying these values, we obtain a resistance of

$$R_v = 1.25 \times 10^9 \ \Omega. \tag{38}$$

Next, we calculate the fractional fluctuations in the tunneling region between the tip and the sample using the conventional $1/f$ formula

$$S_{\frac{\delta R_v}{R_v}}(f) = \frac{4\alpha}{3\pi f N}\frac{(\Delta v)^2}{c^2}. \tag{39}$$

Using the expression derived above for the carrier velocity in the vacuum space along with $N = 1$, we have

$$S_{\frac{\delta R_v}{R_v}} = \frac{4.8 \times 10^{-8}}{f}. \tag{40}$$

Finally, the spectral density of resistance fluctuations in the vacuum is obtained by multiplying by the square of the tunneling resistance

$$S_{\delta R_v}(f) = S_{\frac{\delta R_v}{R_v}} R_v^2 = 7.5 \times 10^{10}\frac{\Omega^2}{f}. \tag{41}$$

V. SAMPLE NOISE CONTRIBUTION CALCULATION

The sample in Koslowski's experiment [12] is a silver film, thickness 50 nm, which has been evaporated onto a silicon wafer. Again, we refer to the following tabulated values for the silver film sample

As in the calculation for the tungsten tip (Table III), the concentration of current carriers within the silver sample must be calculated to reveal the dominant form of 1/f noise in the region. The number of carriers N in the silver film is equal to the concentration times the total volume, and can be written in integral form as

$$N = \int n_{\text{Ag}} \cdot dV. \tag{42}$$

The concentration n_{Ag} for the sample is again the product of the density, the inverse atomic mass and Avogadro's number, which gives the concentration in atoms per cubic meter. The concentration for silver is found to be $n_{\mathrm{Ag}} = 5.86\times10^{28}$ molecules per cubic meter. Next, we calculate the differential volume element in the silver region $dV = Adr$. However, here the geometry is the half plane, so the solid angle is simply

$$\Omega^s = \iint \frac{\widehat{n}\cdot da}{r^2} = \iint \sin\theta d\theta d\varphi = 2\pi. \tag{43}$$

The volume element is then

$$dV^s = Adr = (\Omega r^2)dr = 2\pi r^2 dr. \tag{44}$$

Thus, the average number of carriers in the silver sample directly beneath the tunneling region is given by

$$\langle N\rangle^s = \int dV\cdot n_{\mathrm{Ag}} = \int_{r_i}^{r_f} 2\pi r^2 dr\cdot n_{\mathrm{Ag}} \tag{45}$$

where r_i, the initial tunneling radius within the silver sample, is set to 1 Angstrom, about twice the classical radius of the electron, and r_f represents the maximum tunneling distance through the silver sample, which is just the thickness of the film itself. The integration yields

$$\langle N\rangle^s = 2\pi\cdot n_{\mathrm{Ag}}\frac{1}{3}\left(r_f^3 - r_i^3\right) = 1.5\times10^7 \text{ atoms}. \tag{46}$$

Then, the number of carriers per unit length is found by dividing by the thickness of the silver sample

$$N' = \frac{N}{r_f} = 3.1\times10^{14}\ \frac{\text{molec}}{m}. \tag{47}$$

Again, we encounter within the silver sample a large number of carriers, indicating that the coherent form of Q1/f noise also dominates this region. However, again the geometry of the region directly beneath the tunneling point must be given careful treatment. Directly beneath the point of tunneling, the carriers first enter a very small fraction of the silver sample and eventually spread throughout the thickness of the film. For this region, we should again proceed to calculate the spectral density of resistance fluctuations using the generalized Q1/f formula and the coherence parameter s. In the silver film, the coherence parameter is $s = 2r_0N' = 1.75$.

Calculating the "spreading resistance" in the silver sample, using the resistivity ρ_{Ag} and integrating over consecutive "shells" of increasing radial distance from the tunneling point, we obtain the resistance in the silver sample

$$R_s = \int \frac{\rho_{\mathrm{Ag}}dr}{A} = \int_{r_i}^{r_f}\frac{\rho_{\mathrm{Ag}}dr}{2\pi r^2} = 25.25\,\Omega. \tag{48}$$

Again, we start with the general expression for the spectral density of resistance fluctuations, given by

$$S_{\delta R_s}(f) = \frac{1}{1+s}S^{\mathrm{conv}}_{\frac{\delta R_s}{R_s}}(f)\cdot R_s^2 + \frac{s}{1+s}S^{\mathrm{coh}}_{\frac{\delta R_s}{R_s}}(f)\cdot R_s^2. \tag{49}$$

Within the silver sample, we have

$$dN = dV\cdot n_{\mathrm{Ag}} = 2\pi r^2 dr\cdot n_{\mathrm{Ag}} \tag{50}$$

and the coherence parameter is

$$s = 2r_0\frac{n_{\mathrm{Ag}}dV}{dr} = 4\pi r_0 n_{\mathrm{Ag}} r^2. \tag{51}$$

Now, our expression for the spectral density can be written

$$S_{\delta R_s}(f) = \frac{\rho_{\mathrm{Ag}}^2\alpha\left(\frac{\Delta v}{c}\right)^2}{f6\pi^4 n_{\mathrm{Ag}}}\int_{r_i}^{r_f}\frac{dr}{[1+Mr^2]r^6} + \frac{\rho_{\mathrm{Ag}}^2\alpha r_0}{f\pi^3}\int_{r_i}^{r_f}\frac{dr}{[1+Mr^2]r^4} \tag{52}$$

where we have simplified the integral by setting $M = 4\pi r_0 n_{\mathrm{Ag}}$. Once again, the integral is simplified by considering two cases; when r is very small, directly beneath the point of tunneling, and when r is large, when the tunneling electrons have traveled completely through the thickness of the silver sample. For the case when r is small, the denominator of the first integral is dominated by the r^6 factor, just as in the tungsten tip. When r is very large, the denominator of the second integral is dominated by the r^4 factor. Therefore, the above equation is simplified by dropping the $[1 + M\ r^2]$ factor from the denominators completely, leaving

$$S_{\delta R_s}(f) = \frac{\rho_{\mathrm{Ag}}^2\alpha\left(\frac{\Delta v}{c}\right)^2}{f6\pi^4 n_{\mathrm{Ag}}}\int_{r_i}^{r_f}\frac{dr}{r^6} + \frac{\rho_{\mathrm{Ag}}^2\alpha r_0}{f\pi^3}\int_{r_i}^{r_f}\frac{dr}{r^4}. \tag{53}$$

In the silver sample, just as in the tip, we assume random collisions of the carriers with the lattice

$$\left(\frac{\Delta v}{c}\right)^2 = \frac{6k_BT}{m^*c^2} = 2.9\times10^{-6} \tag{54}$$

where m^* is the effective mass of the charge carrier in silver, for simplicity we have set $m^* = 0.1m_e$, which is an average value for the effective mass of the electron in most conducting materials. With all of the parameters defined, integrating the expression of the spectral density yields

$$S_{\delta R_s}(f) = \frac{3.1\times10^{-6}\,\Omega^2}{f} + \frac{5.6\times10^{-5}\,\Omega^2}{f}. \tag{55}$$

Again, the second term, the coherent contribution dominates in the silver sample region. The fractional fluctuation in resistance is obtained by dividing the spectral density by the squared sample resistance

$$S_{\frac{\delta R_s}{R_s}}(f) = S_{\delta R_s}\cdot R_s^{-2} = \frac{8.8\times10^{-8}}{f}. \tag{56}$$

VI. Total Circuit Resistance Fluctuations

Finally, the expression for the total spectral density of current fluctuations of the three-component system can be constructed involving the coherent and conventional resistance fluctuations from each term. The spectral density of current fluctuations can

TABLE IV
RESISTANCE, FRACTIONAL FLUCTUATIONS, AND SPECTRAL DENSITY

Region	Resistance	Fractional fluctuations	Spectral density
Tungsten tip	14.2Ω	$1.1\text{x}10^{-10}$/Hz	$2.2\text{x}10^{-8}\Omega^2$/Hz
Vacuum space	$1.25\text{x}10^{9}\Omega$	$4.8\text{x}10^{-8}$/Hz	$7.5\text{x}10^{10}\Omega^2$/Hz
Silver sample	25.25Ω	$8.8\text{x}10^{-8}$/Hz	$5.6\text{x}10^{-5}\Omega^2$/Hz

then provide information about the perceived fluctuations in tip height above the sample. First, we summarize the resistance, fractional fluctuations, and spectral density from each region (Table IV).

The current can be written using Ohm's law. The voltage is set equal to the EMF of the circuit ε and R_{total} is the sum of the resistances of each component since the components are in series with each other

$$I = \frac{\varepsilon}{R_{\text{total}}} = \frac{\varepsilon}{R_t + R_v + R_s}. \tag{57}$$

The variance in the current is then

$$\delta I = \frac{-\varepsilon}{R_{\text{total}}^2}(\delta R_t + \delta R_v + \delta R_s) \tag{58}$$

where δR_t, δR_v, and δR_s are Q1/f resistance fluctuations in the tip, vacuum and sample respectively. The three components are uncorrelated, each contributing independently and, therefore, the cross terms can be dropped when we square the expression

$$(\delta I)^2 = \left(\frac{\varepsilon}{R_{\text{total}}^2}\right)^2 \left[(\delta R_t)^2 + (\delta R_v)^2 + (\delta R_s)^2\right] \tag{59}$$

which is also

$$\left(\frac{\delta I}{I}\right)^2 = \frac{1}{R_{\text{total}}^2}\left[(\delta R_t)^2 + (\delta R_v)^2 + (\delta R_s)^2\right] \tag{60}$$

or, written in terms of the fractional fluctuations of resistance fluctuations

$$S_{\frac{\delta I}{I}}(f) = \left(\frac{R_t}{R_{\text{total}}}\right)^2 S_{\frac{\delta R_t}{R_t}}(f) + \left(\frac{R_v}{R_{\text{total}}}\right)^2 S_{\frac{\delta R_v}{R_v}}(f) + \left(\frac{R_s}{R_{\text{total}}}\right)^2 S_{\frac{\delta R_s}{R_s}}(f) \tag{61}$$

gives an expression for the fractional fluctuations in the current noise as a function of the fractional fluctuations in resistance of each region. This expression is dominated by the middle term, which has the largest coefficient. Plugging in the resistances and fractional fluctuations from the table above, the total fractional fluctuations in the current of the three-component system is then

$$S_{\frac{\delta I}{I}}(f) = \frac{4.8 \times 10^{-8}}{f}. \tag{62}$$

This quantity represents the fractional fluctuations in the current, dominated by fluctuations in the tunneling region. We could, therefore, define the spectral density of the tunneling current noise as

$$S_{\delta I} = I^2 \cdot S_{\frac{\delta I}{I}}(f) = 1.9 \times 10^{-29}\frac{A^2}{f}. \tag{63}$$

Finally, the fractional fluctuations in the current can now be used to give insight into the variations in the tip-sample separation distance, δs_0. Recalling (36) from above, relating current fluctuations with the separation distance

$$\frac{\delta I}{I} = -2\kappa(\delta s_0). \tag{64}$$

Now, plugging in the value for the total current fluctuations and the given value for κ, taken to be 20 nm^{-1}, as in Section III, we can solve for the perceived variation in height due to current fluctuations

$$\delta s_0 = \frac{\delta I}{I}\frac{1}{2\kappa} = \frac{5.5 \times 10^{-15}\, m}{\sqrt{\text{Hz}}}. \tag{65}$$

VII. CONCLUSION

In the theoretical Q1/f calculation of the current noise, the dominant term was found to be the noise from the tunneling current. The corresponding current fluctuations δI are defined as

$$\left\langle (\delta I)^2 \right\rangle_f = S_{\delta I}(f) \tag{66}$$

which gives a theoretical value of current fluctuations of

$$\delta I = \sqrt{S_{\delta I}} = 4.3 \times 10^{-15}\,\frac{\text{A}}{\sqrt{\text{Hz}}}. \tag{67}$$

The experimental data of Koslowski [12] for the magnitude of the tunneling current noise was obtained by two methods; using a digital signal analyzer connected to the current signal to precisely measure the spectral behavior and using a crude "noisemeter" consisting of two independent channels that evaluate the noise magnitude at two specific frequencies $\text{f}_1 = 2.3$ kHz and $\text{f}_2 = 4.7$ kHz. These two frequencies were chosen to be well above the cutoff frequency of the topographic feedback loop to avoid interference from the current noise and other properties of the feedback loop, such as the tunneling barrier height. Each channel of the "noisemeter" calculates the noise magnitude by passing the current signal through a bandpass filter. The filter signal is then squared and averaged over a time interval switchable between about 30 or 300 ms. The output signal of the "noisemeter" is proportional to the power spectral density of the current noise at 2.3 or 4.7 kHz.

The experiments were done on thin silver films deposited onto silicon. In surface images, the bright areas were defined as regions of high current noise (later referred to as S regions) embedded in darker regions of low current noise (M regions). At the 2.3 kHz frequency, the spectral density of current noise in the M regions was approximately $S_1 = 1.2\times10^{-27}\ A^2/\text{Hz}$ and in the S regions approximately $S_1 = 2 \times 10^{-25}\ A^2/\text{Hz}$. The corresponding noise amplitudes are obtained by taking square roots, as above, giving the current fluctuations δI. In the low

noise regions, this gives $\delta I = 3.5 \times 10^{-14}$ and for high noise regions $\delta I = 4.5 \times 10^{-13}$.

The theoretical noise amplitudes are fairly close to the observed values in the low noise regions of the sample, within one order of magnitude. The theoretical values obtained were based on geometrical parameters that were estimated, such as tip geometry, tip-sample separation distance, and current set by the feedback loop.

The achievable THz spectral resolution is therefore, as mentioned in the abstract, $\Delta\omega/\omega = [2\mathrm{C}\ln 2]^{1/2} = [2\ln 2(S_R/R^2)/4Q_l^4]^{1/2} = [1.66 \cdot 10^{-12}]^{1/2} = 1.3\ 10^{-6}$. This expression allows for the optimization of the system by optimizing the factors contained in the expression of S_R/R^2.

For instance, the noise is reduced if the velocity change of the electrons in the tunneling process is lowered, thereby reducing the bremsstrahlung amplitude of this process. This amplitude determines the conventional part of Q1/f noise. It also would be useful to increase the number of electrons involved in tunneling at any time, so N would be larger than 1 in (39) and (40). A reviewer has suggested the use of a gas instead of vacuum, in order to increase N. This, however, introduces other forms of noise caused by the fluctuating number of adsorbed gas molecules on the sample and tip surfaces. If this problem could be overcome with the use of noble gases, the formation of space charge would also help to reduce noise. This would in fact sacrifice lateral spatial STM resolution for sharper spectral sensing of chemical and biological agents.

We finally mention that the data characterizing various STM systems could differ very much from what we used as an example. For instance, if instead of using $k = 20/\mathrm{nm}$ in the exponent of the tunneling transmission factor we would use the higher value of 25/nm, the vacuum resistance would increase its exponent of 9 by about 20%, i.e., the current would decrease by almost two orders of magnitude. On the other hand, a tenfold increase in the quality factor of 10 that was assumed at THz frequencies would decrease the frequency uncertainty $\Delta\omega/\omega$ by two orders of magnitude.

ACKNOWLEDGMENT

REFERENCES

[1] P. H. Handel, "1/f noise-an 'infrared' phenomenon," *Phys. Rev. Lett.*, vol. 34, p. 1492, 1975.

[2] P. H. Handel, "Nature of 1/f phase noise," *Phys. Rev. Lett.*, vol. 34, p. 1495, 1975.

[3] P. H. Handel, "Quantum approach to 1/f noise," *Phys. Rev.*, vol. 22A, p. 745, 1980.

[4] P. H. Handel, "Quantum theory of 1/f noise," *Phys. Lett.*, vol. 53A, p. 438, 1975.

[5] P. H. Handel, "Coherent and conventional quantum 1/f effect," *Phys. Stat. Sol. (b)*, vol. 194, p. 393, 1996.

[6] A. van der Ziel, "Unified presentation of 1/f noise in electronic devices; Fundamental 1/f noise sources," *Proc. IEEE*, vol. 76, pp. 233–258, 1988.

[7] A. van der Ziel, "Semiclassical derivation of Handel's expression for the hooge parameter," *J. Appl. Phys.*, vol. 63, pp. 2456–2457, 1988.

[8] A. van der Ziel, "The experimental verification of Handel's expressions for the hooge parameter," *Solid State Electron.*, vol. 31, pp. 1205–1209, 1988.

[9] P. H. Handel, "Fundamental quantum 1/f noise in small semiconductor devices," *IEEE Trans. Electr. Devices*, vol. 41, pp. 2023–2033, 1994.

[10] P. H. Handel, "Noise, low frequency," in *Wiley Encyclopedia of Electrical and Electronics Engineering*, J. G. Webster, Ed. New York: Wiley, 1999, vol. 14, pp. 428–449.

[11] P. H. Handel and A. G. Tournier, "Nanoscale engineering for reducing phase noise in electronic devices," *Proc. IEEE*, vol. 93, no. 10, pp. 1784–1814, Oct. 2005.

[12] B. Koslowski, "1/f noise in scanning tunneling microscopy," in *Proc. VI. Van der Ziel Symp. Quantum 1/f Noise and Other Low Frequency Fluctuations in Electronic Devices*, P. H. Handel and A. L. Chung, Eds., 1996, vol. #371, Amer. Inst. Physics Proc., p. 149.

[13] A. M. Truong, P. H. Handel, and B. Henning, Quantum 1/f Noise in Gold Nanocluster Chemiresistor Sensors submitted to a subsequent issue of this Journal.

Amanda M. Truong received the B.S. and M.S. degrees in physics from the University of Missouri, St. Louis. Currently, she is working towards the Ph.D. degree at the Physics Department, University of Missouri, concentrating on quantum 1/f noise in optical detectors, STM noise limitations, and electronic nose sensor systems.

Peter H. Handel (M'85–SM'90) received the M.S. degree in atomic and theoretical physics and the Ph.D. degree in solid-state theory in 1965, both from the University of Bucharest, Bucharest, Romania.

From 1960 to 1967, he was a Scientist at the Institute of Physics, Romanian Academy, Bucharest. During 1967–1969, he was a Scientist at the Max V. Laue-Paul Langevin Institute, Munich, Germany. He has been a Professor of Physics at the University of Missouri, St. Louis, since 1969. He developed the quantum theory of 1/f noise in 1975, and researched the infrared divergence effect of 1/f fluctuations in physical cross sections and process rates. In 1981, he developed a polarization catastrophe theory of atmospheric electricity. He is also a founding member of the Center for Molecular Electronics, University of Missouri, St. Louis. Since 2001 he was also member of the ultra-low phase noise Multidisciplinary University Research Initiative at University of California, Santa Barbara. He has also made contributions to solid-state, plasma and electronic noise theory. The simple coherent and conventional quantum 1/f effect formulae are applicable to noise and phase noise in most high-technology materials, devices and systems, particular useful in nanotechnology, MEMS, and spintronics.

Dr. Handel has been organizer and Chairman of the Quantum 1/f Symposia since 1990.

Phil Fraundorf is currently a faculty member in physics and astronomy at the University of Missouri, Saint Louis. He's enjoyed being a regional scientific observer of extraterrestrial, electronic, and other materials for nanoscopic investigation that have "walked in the door." He's also worked at offering nanoscale exploration tools for industry and university researchers around the midwest, implementing mathematical techniques for exploration of solids on the atomic scale, and developing tools for recognizing subsystem correlation on multiple scales of time and space and organization.